Pressure effect on crystallization of $Zr_{41}Ti_{14}Cu_{12.5}Ni_{10}Be_{22.5}$ bulk metallic glass prepared by shock-wave quenching

2008 J. Phys.: Condens. Matter 20 015201

(http://iopscience.iop.org/0953-8984/20/1/015201)

J. Phys.: Condens. Matter **20** (2008) 015201 (5pp) doi:10.1088/0953-8984/20/01/015201

Pressure effect on crystallization of $Zr_{41}Ti_{14}Cu_{12.5}Ni_{10}Be_{22.5}$ bulk metallic glass prepared by shock-wave quenching

C Yang[1,2], W P Chen[1], R P Liu[2], Z J Zhan[2], M Z Ma[2], W K Wang[2], X D Wang[3], Q P Cao[3], J Z Jiang[3], C Lathe[4] and H Franz[4]

[1] Key Laboratory for Advanced Metallic Materials Processing, School of Mechanical Engineering, South China University of Technology, Guangzhou 510640, People's Republic of China
[2] State Key Laboratory of Metastable Materials Science and Technology, Yanshan University, Qinhuangdao 066004, People's Republic of China
[3] Laboratory of New-Structured Materials, Department of Materials Science and Engineering, Zhejiang University, Hangzhou 310027, People's Republic of China
[4] HASYLAB am DESY, Notkestrasse 85, D-22603 Hamburg, Germany

E-mail: cyang@scut.edu.cn and wkwang@ysu.edu.cn

Received 6 July 2007, in final form 11 October 2007
Published 29 November 2007
Online at stacks.iop.org/JPhysCM/20/015201

Abstract
Crystallization of $Zr_{41}Ti_{14}Cu_{12.5}Ni_{10}Be_{22.5}$ bulk metallic glass (BMG) prepared by shock-wave quenching under high-temperature and high-pressure has been examined by *in situ* synchrotron radiation x-ray diffraction. The first precipitated phase is found to be the same at different pressures, but the subsequent phase precipitation sequences are different. The crystallization temperature of the BMG increases with pressure, but with a sudden drop at about 6.0 GPa. The different phase precipitation sequences and the sudden drop in the crystallization temperature can be explained by complex pressure effects on the atomic configuration of the BMG.

1. Introduction

The structure of materials is profoundly altered under high pressure due to large changes in atom spacing, chemical bonding and Gibbs free energy [1]. There are various forms of structural transition, or phase transition, for materials under static and dynamic high pressure [2, 3]. For the new materials family of $Zr_{41}Ti_{14}Cu_{12.5}Ni_{10}Be_{22.5}$ bulk metallic glass (BMG), which are of high thermal stability and have great potential for engineering applications, the phase transition, or crystallization process, under static high pressure can pass through different sequences [4–10]. In addition to the crystallization sequence, or phase precipitation sequences, the phase precipitation onset temperature, or crystallization temperature (T_x), during crystallization of the BMG may even be further influenced by pressure. It was reported that pressure can restrain crystallization and increase T_x of the BMG, because the long-range atomic transport required for crystallization is retarded by pressure [5]. In this case, T_x increases greatly with pressure, while the crystallization sequence is the same for different pressures. The influence of pressure on the crystallization sequence has also been proved experimentally [7, 9]. In a such case, pressure can change both the crystallization sequence and T_x, because changed crystallization sequences (different initially precipitated phases) can cause a decrease in T_x. Recently, our group and co-workers found that the initial precipitated phase of the BMG is the same at pressure, but subsequent crystallization sequences are different [10]. Furthermore, its T_x increases with pressure, but with a sudden drop at the pressure of a subsequent changed crystallization sequence.

For a long time, melt quenching, such as water-quenching and copper mold casting, has been the main method of preparation of BMGs. This method is mainly related to the variable of temperature. Apart from temperature, static high pressure has also been reported to be favorable for glass formation [11]. Considering that dynamic high pressure can melt a metallic alloy instantly, dynamic

high pressure, or shock-wave quenching, was invented to prepare $Zr_{41}Ti_{14}Cu_{12.5}Ni_{10}Be_{22.5}$ BMG [12]. Furthermore, it was reported that shock-wave-quenched BMGs possess different crystallization sequences compared with those of water-quenched ones under continuous heating and ambient pressure [13]. From a theoretical point of view, therefore, it is of great interest to know what crystallization sequence a shock-wave-quenched BMG will present, and whether it exhibits different crystallization sequences in comparison with those of a water-quenched one or not under static high pressure and continuous heating. Whether its T_x drops at high pressure or not is also a particularly interesting question.

In the present work, crystallization of $Zr_{41}Ti_{14}Cu_{12.5}Ni_{10}Be_{22.5}$ BMG prepared by shock-wave quenching is investigated under high temperature and high pressure by *in situ* synchrotron radiation x-ray diffraction. It is expected that this may provide farther insight into the physical nature of dynamic and static high-pressure effects on the crystallization sequence and temperature of the BMG.

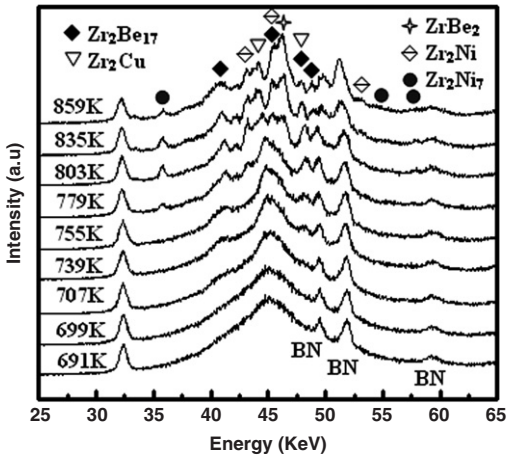

Figure 1. *In situ* EDXRD patterns recorded at various temperatures for WQ-SWQ $Zr_{41}Ti_{14}Cu_{12.5}Ni_{10}Be_{22.5}$ BMG at 0.3 GPa (Ed = 108.03 keV Å). The fluorescence peaks, located in the energy range 31–34 keV, and a few Bragg peaks from BN were detected.

2. Experiments

The $Zr_{41}Ti_{14}Cu_{12.5}Ni_{10}Be_{22.5}$ BMG was prepared by water-quenching and shock-wave quenching [12]. First, the BMG was prepared by water-quenching. Then, the water-quenched BMG was quenched again into the glass state by shock-wave quenching at a shock pressure of 100 GPa. The water-quenched and shock-wave-quenched (WQ-SWQ) sample was cut out from the recovery device, ground and polished for experimental analyses. The amorphous nature of the samples before and after shock-wave quenching was verified with x-ray diffraction, transmission electron microscopy and differential scanning calorimetry. The composition of the WQ-SWQ sample was examined by the inductively coupled plasma–atomic emission spectroscopy method to be the same as the water-quenched BMG within experimental uncertainty.

In situ high-temperature and high-pressure energy-dispersive x-ray diffraction (EDXRD) patterns for the WQ-SWQ BMG were recorded using synchrotron radiation at HASYLAB in Hamburg, Germany, by a multi-anvil pressure apparatus [14, 15] with 8 mm^3 pressure cells at the MAX 80 station. The sample assembly and experimental procedures are shown in [10]. The cubic sample assembly and multi-anvil pressure apparatus used by us guarantee that temperature and pressure inhomogeneities within the powder samples cannot exert detectable influences on the crystallization sequence of the BMG sample. The temperature was measured by means of a thermocouple close to the powder sample with a stability of ± 1 K. The pressure of the sample was calculated from the lattice constant of NaCl using the Decker equation of state [16]. In each run of the experiment, the sample was first compressed to a certain pressure at room temperature and then isobarically heated up to 889 K in steps of 8 K with a recorded EDXRD pattern every 4 min in order to observe the onset T_x in the pressure range up to 6.5 GPa. Pure Zr, Fe and the WQ-SWQ BMG powders were used to examine the possible oxidation of samples during the heating treatments using the high-pressure sample assembly. It was found that only pure metallic phases in these three systems were detected after heating treatment at temperatures up to 889 K under pressure.

3. Results and discussion

It is found that the applied pressure strongly affects the crystallization sequences and T_x of the WQ-SWQ BMG. Under pressures up to 6.5 GPa the primarily precipitated phase is Zr_2Be_{17}, but the subsequent crystallization sequences are different. The crystallization sequences are mutually different at pressure below 1.5 GPa, from 2.1 to 5.4 GPa and about 6.0 GPa, respectively.

Figure 1 shows the EDXRD patterns recorded for the sample at 0.3 GPa and at various temperatures. A broad amorphous peak, located at about $E = 45$ keV, together with Bragg peaks from BN and fluorescence peaks in the energy range of 31–33.5 keV, is observed in the patterns recorded at each temperature. A new tiny crystalline peak ($E = 41.0$ keV) from the Zr_2Be_{17} phase appears at 707 K. With the increased temperature, another diffraction peak ($E = 47.9$ keV) from the Zr_2Be_{17} phase is observed at 739 K. At 755 K, the crystalline peak ($E = 44.7$ keV) from Zr_2Cu crystal is detected. With the continuously increased temperature, the sample exhibits a different crystallization sequence relative to the water-quenched BMG [10]. Compared with the precipitated $ZrBe_2$ phase after the Zr_2Cu phase for the water-quenched BMG, the Zr_2Cu crystal of the sample is followed by precipitated Zr_2Ni ($E = 43.1$, 45.4 and 53.3 keV) and Zr_2Ni_7 ($E = 35.8$ and 57.7 keV) phases at 779 K. With further increase in the temperature, the peak from $ZrBe_2$ phase, located at $E = 46.3$ keV, is recorded at 803 K. After that, the diffraction peak intensity from the precipitated phases increases continuously. Up to 889 K, no crystalline peaks from other new phases are found. The crystallization sequence of the sample at 1.5 GPa is the same as that at 0.3 GPa. Figure 2 shows the EDXRD patterns recorded for the sample at 1.5 GPa and at various temperatures. The primary crystalline peak ($E = 41.7$ keV)

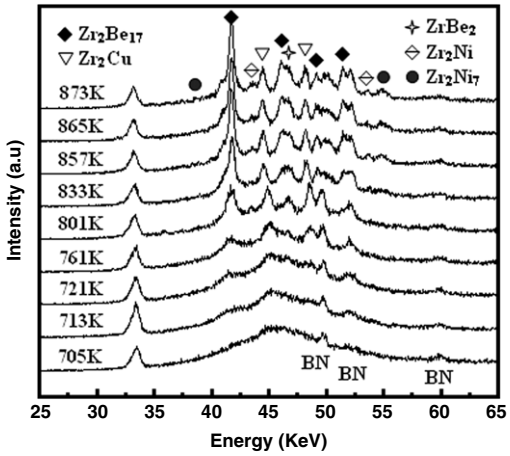

Figure 2. *In situ* EDXRD patterns recorded at various temperatures for WQ-SWQ $Zr_{41}Ti_{14}Cu_{12.5}Ni_{10}Be_{22.5}$ BMG at 1.5 GPa (Ed = 108.19 keV Å). The fluorescence peaks, located in the energy range 32–34 keV, and a few Bragg peaks from BN were detected.

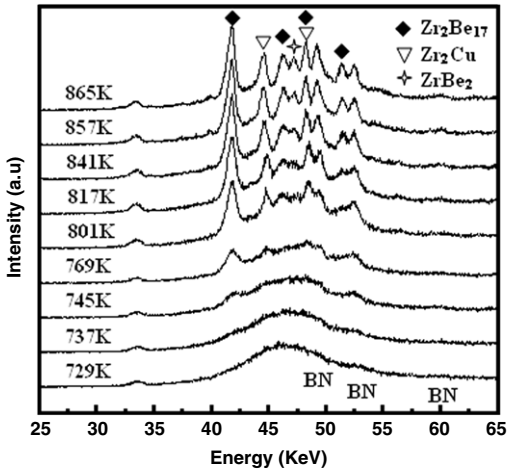

Figure 3. *In situ* EDXRD patterns recorded at various temperatures for WQ-SWQ $Zr_{41}Ti_{14}Cu_{12.5}Ni_{10}Be_{22.5}$ BMG at 2.1 GPa (Ed = 107.82 keV Å). The fluorescence peaks, located in the energy range of 32–35 keV, and a few Bragg peaks from BN were detected.

from the Zr_2Be_{17} phase appears at 713 K, followed by the appearance of the peak (E = 44.5 keV) of the Zr_2Cu phase at 761 K. At 801 K, the new peaks from Zr_2Ni (E = 43.5, 46.2 and 53.6 keV) and Zr_2Ni_7 (E = 38.7 and 54.9 keV) emerge. With the further increase in the temperature, the peak (E = 46.8 keV) from the $ZrBe_2$ phase begins to appear at 857 K, accompanied by the emergence of other peaks of the precipitated phases.

The crystallization sequences of the sample are the same in the pressure range from 2.1 to 5.4 GPa. Figure 3 shows the EDXRD patterns recorded at 2.1 GPa and at various temperatures. The primary precipitated phase is also Zr_2Be_{17}; its diffraction peak (E = 41.8 keV) is observed at 737 K. With the increased temperature, the peaks (E = 44.8 and 48.4 keV) from the Zr_2Cu phase and another peak (E = 48.4 keV) from the Zr_2Be_{17} phase are detected at 769 K. With the further increased temperature, instead of a Zr_2Cu phase followed by

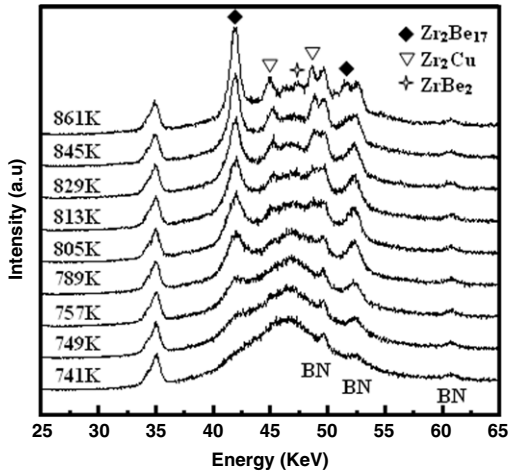

Figure 4. *In situ* EDXRD patterns recorded at various temperatures for WQ-SWQ $Zr_{41}Ti_{14}Cu_{12.5}Ni_{10}Be_{22.5}$ BMG at 4.6 GPa (Ed = 107.76 keV Å). The fluorescence peaks, located in the energy range of 33–36 keV, and a few Bragg peaks from BN were detected.

Zr_2Ni and Zr_2Ni_7 phases for the sample below 1.5 GPa, a new peak (E = 47.2 keV) from the $ZrBe_2$ phase is observed at 817 K after the precipitation of the Zr_2Cu phase. Figure 4 further verifies that the crystallization sequence at 4.6 GPa is the same as that at 2.1 GPa. The primary crystalline peak (E = 42.0 keV) from the Zr_2Be_{17} phase appears at 749 K, followed by the appearance of the peak (E = 45.1 and 48.8 keV) of the Zr_2Cu phase at 813 K. At 861 K, the peak (E = 47.3 keV) from the $ZrBe_2$ phase begins to appear.

It is interesting to note that the T_x of the sample drops suddenly at 6.0 GPa, which is similar to the drop in T_x of the water-quenched BMG at 5.6 GPa. However, its crystallization sequence at 6.0 GPa is different from both those at other pressures and that of the water-quenched BMG at 5.6 GPa, respectively. Figure 5 shows the EDXRD patterns recorded at 6.0 GPa and at various temperatures. It is found that the primary precipitated phase for the sample is still Zr_2Be_{17}, but the peak (E = 42.2 keV) appears at 721 K. This indicated that its T_x at 6.0 GPa is 40 K lower than that at 5.4 GPa. Up to 809 K, the peak (E = 45.0 keV) from the ZrNi phase is recorded. With the increased temperature, the new peaks from the metastable fcc-$NiZr_2$ phase (E = 46.4 keV) [17], the $Cu_{10}Zr_7$ phase (E = 46.4 and 48.7 keV) and the $ZrBe_2$ phase (E = 47.8 keV), respectively, are observed simultaneously at 839 K. The precipitation of ZrNi and $Cu_{10}Zr_7$ phases in the present case is possible because of the complex effects of dynamic high pressure on metallic melts during shock-wave quenching and of static high pressure on the crystallization process of the sample. This can be demonstrated by the experimental result under ambient pressure, which reported that precipitation of the ZrNi phase at 725 K was followed by a $Cu_{10}Zr_7$ phase at 873 K from WQ-SWQ BMG prepared at a shock pressure of 120 GPa under continuous heating [18]. In addition, the precipitation of a $Cu_{10}Zr_7$ phase in our case may be related to depletion of Be and Zr at lower temperatures. No new phases are detected with further increased temperature up to 889 K.

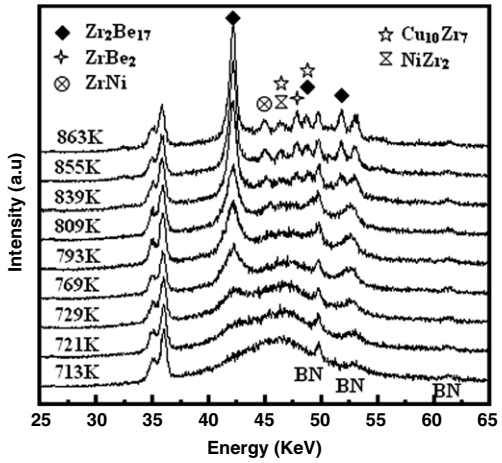

Figure 5. *In situ* EDXRD patterns recorded at various temperatures for WQ-SWQ $Zr_{41}Ti_{14}Cu_{12.5}Ni_{10}Be_{22.5}$ BMG at 6.0 GPa (Ed = 107.72 keV Å). The fluorescence peaks, located in the energy range of 34–37 keV, and a few Bragg peaks from BN were detected.

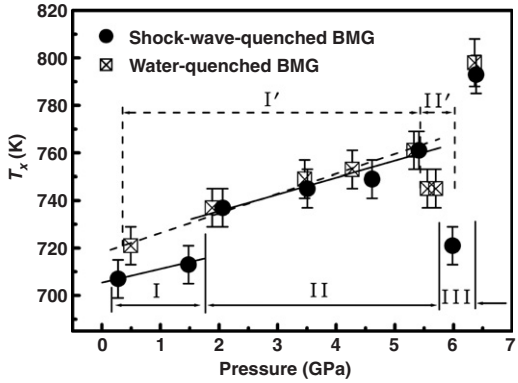

Figure 6. Pressure dependence of crystallization temperature for WQ-SWQ $Zr_{41}Ti_{14}Cu_{12.5}Ni_{10}Be_{22.5}$ BMG. The data for water-quenched BMG were derived from [10].

In our present experiments, the primary precipitated phases of all the samples are Zr_2Be_{17} at all the applied pressures. Nevertheless, the subsequent phase precipitation sequences are different, as indicated in figures 1–5. According to the difference in the crystallization sequences, the pressure dependence of T_x for the sample can be divided into three regions, as shown in figure 6. For comparison, the pressure dependence of T_x for the water-quenched BMG is also presented [10], and can be divided into two regions. In the different pressure regions, the crystallization sequences for the sample are shown below.

In region I, in which the applied pressure is lower than 1.5 GPa, the crystallization sequence is Am. $\rightarrow$ Am.$'$ + Zr_2Be_{17} $\rightarrow$ Am.$''$ + Zr_2Be_{17} + Zr_2Cu $\rightarrow$ Am.$'''$ + Zr_2Be_{17} + Zr_2Cu + Zr_2Ni + Zr_2Ni_7 $\rightarrow$ Am.$''''$ + Zr_2Be_{17} + Zr_2Cu + Zr_2Ni + Zr_2Ni_7 + $ZrBe_2$. This is the same as that in region II$'$ for the water-quenched BMG. In region II, in which the applied pressure is from 2.1 to 5.4 GPa, the crystallization sequence is Am. $\rightarrow$ Am.$'$ + Zr_2Be_{17} $\rightarrow$ Am.$''$ + Zr_2Be_{17} + Zr_2Cu $\rightarrow$ Am.$'''$ + Zr_2Be_{17} + Zr_2Cu + $ZrBe_2$. This is the same as that in region I$'$ for the water-quenched BMG. In region III, in which the applied pressure is about 6.0 GPa, the crystallization sequence is Am. $\rightarrow$ Am.$'$ + Zr_2Be_{17} $\rightarrow$ Am.$''$ + Zr_2Be_{17} + ZrNi $\rightarrow$ Am.$'''$ + Zr_2Be_{17} + ZrNi + $NiZr_2$ + $Cu_{10}Zr_7$ + $ZrBe_2$.

Due to the different crystallization sequences, the slope of the increase of the T_x with pressure is different in different pressure regions. In region I, the slope is 5.0 K GPa^{-1}, lower than the 8.1 K GPa^{-1} for the water-quenched BMG. The slope in region II is 6.6, 1.5 K GPa^{-1} lower than that of the water-quenched BMG. Like the drop in T_x at about 5.6 GPa for the water-quenched BMG, T_x also drops at about 6.0 GPa in the present case, as shown in figure 6. This indicates that preparation parameters, such as pressure and cooling rate, are independent of the drop in T_x for $Zr_{41}Ti_{14}Cu_{12.5}Ni_{10}Be_{22.5}$ BMG. Considering experimental errors induced by pressure calibration and experimental devices, it is reasonable to believe that the drop in T_x is at the same pressure as for the BMGs prepared by water-quenching and the shock-wave quenching.

In shock-wave quenching [12], metallic alloys were treated by dynamic high pressure in an extremely short time, superheated to melting at an extremely high heating rate, overheated by an extremely high temperature, and then solidified into glass states. Different short-range orders were obtained for the BMGs prepared by shock-wave quenching and water-quenching, respectively [19]. Consequently, the WQ-SWQ BMG possesses different crystallization sequences relative to the water-quenched one in our case. Generally, T_x for metallic glasses increases with pressure because of depression of mobility of atoms by pressure. However, Sun *et al* reported that pressure can change the original atomic configuration of metallic glasses [20]. In particular, Ma *et al* recently demonstrated that pressure can induce transition between two distinct amorphous polymorphs in metallic glass, which is attributed to their different electronic and atomic structures [21]. These discoveries may offer new evidence for understanding the drop of the T_x at 6.0 GPa and different crystallization sequences at different pressures for the WQ-SWQ $Zr_{41}Ti_{14}Cu_{12.5}Ni_{10}Be_{22.5}$ BMG.

It should be noticed that when we utilize a large volume press to investigate the phase transition of materials by *in situ* synchrotron radiation x-ray diffraction under high temperature and high pressure, special attention must be paid to the effect on phase transition of temperature and pressure inhomogeneities within the samples. In our present experiments, a cylindrical boron nitride container with 1 mm inner diameter was used; the center of the container was filled with the BMG powder sample [10, 15]. The powder sample has small volume, at least in the middle of sample, in a range of 0.2 mm along the vertical direction. The cubic sample assembly with a length of a side of 8 mm is compressed by six tungsten carbide anvils in a large hydraulic press. Under these conditions, the temperature fluctuation within the samples is smaller than 10 K in the temperature range used in the present study. At the same time, we try to keep the same experimental conditions, e.g. the distance between thermocouple in the middle to the probing spot, the same probing beam size, the same heating rate, the same assembly setup, the same batch of sample, the only difference is the pressure. Therefore, the effect of temperature inhomogeneities within the samples

on phase transition of the BMG sample can be ignored. Additionally, the BMG powder sample with a size far smaller than those of cubic sample assembly and the anvil faces is compressed by six forces from six tungsten carbide anvils. This guarantees very small pressure inhomogeneity within the powder samples. Because pressures up to 40 GPa did not cause crystallization of $Zr_{41.2}Ti_{13.8}Cu_{12.5}Ni_{10}Be_{22.5}$ BMG at room temperature [6], the effect of pressure inhomogeneity within the samples on phase transition of the BMG sample can also be ignored. On these bases we have tried to study the pressure effect on crystallization behavior of a shock-wave-quenched BMG sample.

4. Conclusion

The static high-pressure effect on crystallization processes and temperature of the WQ-SWQ $Zr_{41}Ti_{14}Cu_{12.5}Ni_{10}Be_{22.5}$ BMG was studied. The same primary precipitated phase but different crystallization processes are found at different pressures. In the pressure range up to 6.5 GPa, crystallization processes for the BMG present three different sequences. Meanwhile, the crystallization temperature increases with pressure, but having different slopes in different pressure regions. At about 6.0 GPa, a sudden drop in the onset crystallization temperature is examined. Both the different crystallization sequences and the sudden drop of the onset crystallization temperature may be due to the differences in atomic configurations at different pressures.

Acknowledgments

The authors would like to thank HASYLAB in Germany for use of the synchrotron radiation facilities. Financial support from Guangdong Natural Science Foundation (no. 07300579), China Postdoctoral Science Foundation (grant no. 20060390198), Postdoctoral Innovation Foundation of South China University of Technology (grant no. 05243), the National Natural Science Foundation of China (grant nos 50731005/50341032), SKPBRC (grant nos 2006CB605201/2007CB616915) and PCSIRT (grant no. IRT0650) is gratefully acknowledged.

References

[1] Somayazula M W, Finger L W, Hemley R J and Mao H K 1996 *Science* **271** 1400
[2] Sharma S M and Sikka S K 1996 *Prog. Mater. Sci.* **40** 1
[3] Duvall G E and Graham R A 1977 *Rev. Mod. Phys.* **49** 523
[4] Sun L L, Wang W K, He D W, Wang W H, Wu Q, Zhang X Y, Bao Z X and Zhao Q 2000 *Appl. Phys. Lett.* **76** 2874
[5] Jiang J Z, Zhou T J, Rasmussen H K, Kuhn U, Eckert J and Lathe C 2000 *Appl. Phys. Lett.* **77** 3553
[6] Jiang J Z, Gerward L and Olsen J S 2002 *Appl. Phys. Lett.* **80** 3015
[7] Sun L L, Kikegawa T, Wu Q, Zhan Z J and Wang W K 2002 *Appl. Phys. Lett.* **80** 3087
[8] Jiang J Z 2002 *Appl. Phys. Lett.* **81** 3894
[9] Sun L L, Kikegawa T, Wu Q, Zhan Z J, Cao L M, Wang L M, Shao G J, Zhang J and Wang W K 2002 *J. Phys.: Condens. Matter* **14** 11243
[10] Yang C, Wang W K, Liu R P, Zhan Z J, Sun L L, Zhang J, Jiang J Z, Yang L and Lathe C 2006 *J. Appl. Phys.* **99** 023525
[11] Wang W H, Wang R J, Dai D Y, Zhao D Q, Pan M X and Yao Y S 2001 *Appl. Phys. Lett.* **79** 1106
[12] Yang C, Liu R P, Zhan Z J, Sun L L, Zhang J, Gong Z Z and Wang W K 2005 *Appl. Phys. Lett.* **87** 051904
[13] Yang C, Zhan Z J, Fan C Z, Liu R P and Wang W K 2007 *Mater. Sci. Eng.* A. **449–451** 617
[14] Shimomura O *et al* 1985 Multi-anvil type x-ray system for synchrotron radiation *Solid State Physics under Pressure* ed S Minomura (Dordrecht: D Reidel Publ. Comp.) p 351
[15] Jiang J Z, Roseker W, Sikorski M, Cao Q P and Xu F 2004 *Appl. Phys. Lett.* **84** 1871
[16] Decker D L 1971 *J. Appl. Phys.* **42** 3239
[17] Altounian Z, Batalla E, Strom-Oisen J O and Walterm J L 1987 *J. Appl. Phys.* **61** 149
[18] Yang C 2005 Short-range order, crystallization kinetics and crystallization process of shock-wave-quenched ZrTiCuNiBe bulk metallic glass effect of shock wave on ZrTiCuNiBe bulk metallic glass *Dissertation for the Doctoral Degree in Engineering* Yanshan University, Qinhuangdao p 71
[19] Yang L, Chao Y, Saksl K, Franz H, Sun L L, Wang W K, Jiang N P, Wu X J and Jiang J Z 2004 *Appl. Phys. Lett.* **84** 4998
[20] Sun L L, Wang W K, Wang L M, Kikegawa T, Wu Q, Zhang J, Fan C Z, Eckert J and Schultz L 2003 *Phys. Rev.* B **68** 052302
[21] Sheng H W, Liu H Z, Cheng Y Q, Wen J, Lee P L, Luo W K, Shastri S D and Ma E 2007 *Nat. Mater.* **6** 192